MAUN Fen Bil. Dergi., 13, 1, 7-14 Araştırma Makalesi/ Research Article
MAUN J. of Sci., 13, 1, 7-14 DOI : 10.18586/msufbd.1612185

Energy and Exergy Analysis of an Absorber Plate With Stainless Steel Scourers

Filiz OZGEN[1], Ayse DAYAN[1], Ugurcan YARDIMCI[2], Celal KISTAK[3] and Nevin CELIK[3]
[1] Firat University, Technology Faculty, 23279 Elazig, Turkey
[2] Bingol University, Vocational School of Technical Sciences, 12100, Bingol, Turkey
[3] Firat University, Department of Mechanical Engineering, 23119 Elazig, Turkey

✉: nevincelik23@gmail.com [1]0000-0003-2278-2093 [2]0000-0001-7056-5574 [3]0000-0001-6511-4058
[4]0000-0003-4621-5405 [5] 0000-0003-2456-5316

Received (Geliş): 03.01.2025 Revision (Düzeltme):14.03.2025 Accepted (Kabul): 29.04.2025

ABSTRACT

In this study, energy and exergy efficiencies of collectors with stainless steel scourers as the surface enhancing elements were evaluated. Three surface types were tested according to the scourers' arrangement. T1 has the highest number of scourers in irregular arrangement. T2 has less scourers in regular row. T3 is the surface without scourers. Experiments were carried out at air flow rates of $\dot{m}$=0,025 kg/s and $\dot{m}$=0,05 kg/s. Ambient temperature, surface temperature, solar radiation, inlet-outlet temperatures of air were measured. The exergy efficiencies at $\dot{m}$=0,025 kg/s kg/s are 50%, 48% and 40%, for T1, T2 and T3, respectively. These values reach up 66%, 55% and 52% at $\dot{m}$=0,05 kg/s, for T1, T2 and T3 respectively. The results show that the flat plate collector (T3) has the lowest efficiency and highest irreversibility. It is also found that the increase in air flowrate improves the collector performance in general.

Keywords: Energy, Exergy, Surface-enhancing elements, Solar Energy Systems, Thermal Performance

Paslanmaz Çelik Telli Bir Yutucu Plakanın Enerji ve Ekserji Analizi

ÖZET

Bu çalışmada, farklı emici yüzey düzenine sahip kolektörlerin enerji ve ekserji verimlilikleri karşılaştırmalı bir analizle değerlendirilmiştir. Emici yüzeyler üzerlerindeki tel yoğunluğuna göre üç tipe ayrılmıştır; düz ve gözeneksiz (T3), orta derecede gözenekli (T2) ve daha karmaşık gözenekli (T1). Deneyler, $\dot{m}$=0,025 kg/s ve $\dot{m}$ =0,05 kg/s hava debisinde gerçekleştirilmiş, çevre sıcaklığı, emici yüzey sıcaklığı, güneş ışınımı, hava giriş-çıkış sıcaklıkları gibi parametreler ölçülmüştür. $\dot{m}$=0,025 kg/s debide T1, T2 ve T3 için enerji verimlilikleri sırasıyla %45, %42 ve %36 olarak elde edilmiştir. $\dot{m}$=0,05 kg/s iken verimliliklerde belirgin artışlar gözlenmiştir. Benzer bir artış eğilimi ekserji verimliliklerinde de gözlenmiştir; $\dot{m}$=0,025 kg/s'de ekserji verimlilikleri sırasıyla %50, %48 ve %40 iken, $\dot{m}$=0,05 kg/s'de bu değerler %66, %55 ve %52'ye ulaşmıştır. Sonuçlar, düz plaka kolektörünün (T3) en düşük verimlilik ve en yüksek tersinmezlikle çalıştığını ortaya koymuştur. Ayrıca, hava debisindeki artışın kolektör performansını genel olarak iyileştirdiği tespit edilmiştir.

Anahtar Kelimeler Enerji, Ekserji, Yüzey Geliştirici Elemanlar, Güneş Enerjisi Sistemleri, Termal Performans

INTRODUCTION

Improving the performance of solar air heaters (SAHs) is a significant focus area in advancing energy systems. To address the challenge, various strategies involving surface modifications have been developed to enhance heat transfer efficiency on absorber surfaces [2–6]. Among these approaches, dual-flow SAHs have emerged as a particularly effective solution, as they substantially increase the heat transfer area, thereby improving thermal performance. Furthermore, incorporating flow-altering obstacles within the air ducts has proven to be a highly effective method for optimizing airflow distribution, which in turn significantly improves the thermal performance of the system [7–9].

The literature presents a wide array of configurations for SAHs, reflecting ongoing efforts to optimize their design and performance. Esen [10] performed comprehensive exergy and energy analyses of SAH systems equipped with obstacle-modified absorber surfaces, evaluating the impact of various obstacle placements on system efficiency. Similarly, Akpinar and Kocyigit [11] conducted experimental investigations on four different absorber surface types, examining their performance under two distinct air mass flow rates to determine optimal operating conditions. Ozgen et al. [12] explored the use of cylindrical tin-can absorber plates in SAHs, systematically testing three different configurations to assess their thermal and aerodynamic performance.
Arabhosseini et al. [13] developed an innovative porous SAH integrated with a recycling system, achieving

notable maximum exergy and energy efficiencies of 22.3% and 63.4%, respectively. Ucar and Inalli [14] investigated the performance of SAHs equipped with graduated plates and fins, revealing that conventional SAHs exhibited the lowest efficiency among the designs studied. Meanwhile, Albizzati [15] conducted an in-depth analysis of porous absorber surfaces, emphasizing their potential to enhance energy gains and improve overall thermal performance.

Karim et al. [16] compared flat sheet, finned, and V-fold SAHs, with V-pleated designs achieving superior efficiency. Moummi et al. [17] demonstrated increased efficiency using rectangular absorber surfaces placed perpendicular to airflow, while Yeh et al. [18] enhanced efficiency and air mass flow rates by employing double-pass fins in reversible flat-layer of SAHs. Sahu and Bhagoria [19] used inclined transverse beams to improve performance, and Alvarez et al. [20] achieved better thermal efficiency with absorber surfaces made of recycled aluminum cans. Kreith and Kreider [21] proposed flow baffles and enlarged heat transfer areas to create turbulence, while Ghoneim [22] emphasized the efficiency benefits of square-section honeycomb configurations.

In this study, thermal performance is improved by integrating stainless steel scourers as surface-modifying elements into solar collectors. The absorber surfaces are categorized as T1, with complex porous arrangements; T2, with scourers in regular rows; and T3, a flat surface without scourers. Energy and exergy efficiencies are employed as primary metrics to evaluate the performance of these designs.

EXPERIMENTAL STUDY

Setup

The experimental design used in this work has been previously applied by the co-authors in earlier research [23, 24], confirming its dependability and suitability for evaluating SAH performance. An graphic illustration of the experimental setup is given in Figure 1. he collector housing has dimensions of 400 mm (height), 800 mm (width), and 1200 mm (length). Insulation is achieved using a 3 cm thick strap layer, while the primary structural framework of the case is constructed from chipboard, a 4 mm thick transparent glass cover is integrated to facilitate solar energy absorption. The collector is positioned with its rear facing south, inclined at a 37° angle to the horizontal plane, ensuring optimal sun exposure for the experimental investigation.

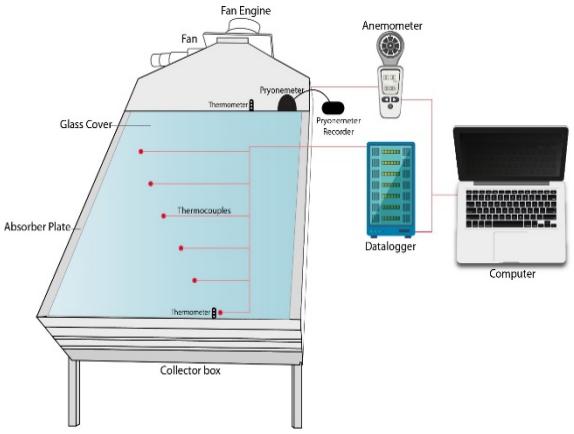

Fig. 1 Schematic of the experimental setup [23, 24]

The absorber surface of a solar air collector is a key component that significantly influences system performance. In order to promote airflow on both sides, this study investigates three potential absorber surface configurations, each of which includes unique surface-enhancing components. It is well established that dual-channel airflow designs can enhance solar collector efficiency [18]. A total of 180 stainless steel scourers were affixed using silicone adhesive to both sides of a 1.5 mm galvanized sheet to create the absorber surfaces. After that, black matte paint was applied to the sheet to maximize its sunlight absorption capabilities.

The first absorber surface (T1) includes 102 stainless steel scourers arranged in a complex and non-uniform pattern, as displayed in Fig. 2a. The second absorber surface (T2) is designed with 78 scourers organized in a structured and uniform layout, as illustrated in Fig. 2b. The third absorber surface (T3), which serves as the flat plate does not have any scourers, as seen in Fig. 2c.

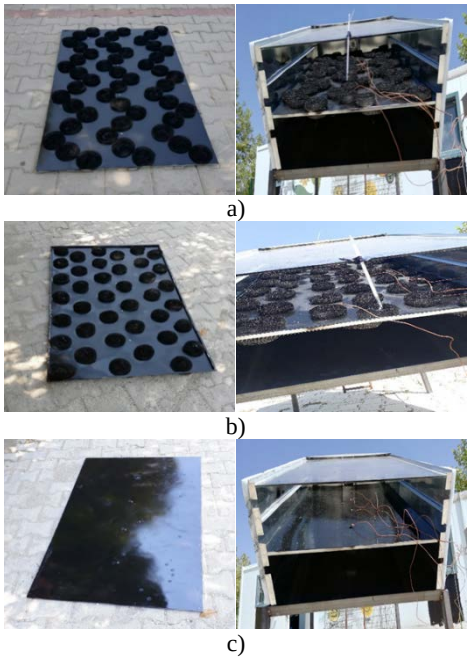

Fig. 2 Absorber surface types **a)** T1, **b)** T2, **c)** T3 [23, 24]

A Pyranometer (Kipp Zonen CM3) is utilized to measure solar radiation. Solar collector is linked to the suction outlet of an air fan (800 m³/h) through a conduit. Airflow was measured using a digital anemometer (AM-4206M) with a metal fan head for improved accuracy. The air temperatures at the collector's outlet and inlet are recorded using a digital thermometer (0-100°C)
To assess temperature distribution on the absorber surfaces, T-type thermocouples are installed at four evenly spaced points, 24 cm apart. Thermocouples are connected to Data Logger (CR 510), which records temperature readings. A manometer is used to measure pressure losses between the outlet and inlet of collector. Additionally, a dimmer is utilized to adjust the mass flow rate at the fan outlet, allowing for effective air suction through the collector, and a rotameter is positioned at the collector's outlet to monitor the mass flow rate.

Data Reduction

The experiments were conducted in Elazığ, Turkey, between 9:00 AM and 4:00 PM, focusing on days with highest observed efficiency. The study involved testing three different absorber surface geometries at two air mass flow rates, $\dot{m}$=0,025 kg/s and $\dot{m}$=0,05 kg/s.
A theoretical model based on unsteady-state conditions was developed based on a thermal energy balance approach [10].

$$[Accumulated\ energy] + [Energy\ gain] = [Absorbed\ energy] - [Lost\ energy]$$

According to the energy balance the equation can be written as follows:

$$\left[mC_p\left(\frac{dT_w}{dt}\right)\right] + \left[\dot{m}C_p(T_o - T_i)\right] = [\eta_0 I A_c] - [U_c(T_w - T_\infty)A_c] \quad (1)$$

where m and $\dot{m}$ represent the mass and mass flow rate of air respectively. C_p is the specific heat capacity of the air. T_w is the average of all measured wall temperatures, T_∞ is the surrounding ambient temperature, T_o and T_i are the air temperatures at the outlet and inlet of the collector, I is the radiation, A_c is the surface area of the collector. The optical yield (η_0) and the energy loss coefficient U_c are the parameters that characterize the behavior of the collector. Note that (η_0) represents the fraction of solar radiation absorbed by the panel and depends mainly on the transmittance of the transparent covers and the absorptivity of the panel [10]. Thermal efficiency η_I of collectors is characterized as the proportion of energy gained to radiation at the collector plane:

$$\eta_I = \dot{m}C_p(T_o - T_i)/(IA_c) \quad (2)$$

The 1st law of thermodynamics lays the groundwork for examining thermal systems' energy balance with an emphasis on energy transfer and conservation. When combined with standard thermal design procedures, the second law of thermodynamics provides a more comprehensive understanding of system performance by addressing the directional nature of energy transformations and irreversibility.
Exergy analysis, integrating the principles of laws of thermodynamics, evaluates not just the amount of energy transferred throughout a system, but also its quality. This approach is essential for identifying thermodynamic inefficiencies and areas of irreversibility, known as exergy losses, in thermal and chemical processes. By highlighting these inefficiencies, exergy analysis aids in minimizing entropy generation and optimizing the performance of energy systems. In this study, the solar collector is analyzed as a closed system under several assumptions: steady-state flow, negligible kinetic and potential energy effects, air behaving as an ideal gas with constant specific heat, and positive directions for heat transfer to the system and work transfer from the system. These assumptions simplify the analysis while providing valuable insights into system performance and efficiency. The mass conservation is:

$$\Sigma\dot{m}_i = \Sigma\dot{m}_o \quad (3)$$

The overall energy and exergy balance can be expressed as follows [14]:

$$\sum \dot{E}x_i - \sum \dot{E}x_o = \sum \dot{E}x_{dest} \quad (4)$$

where the subscripts i, o and $dest$ represent the inlet, outlet and destructed terms respectively. then the exergy balance including heat, work and mass flows can be written as:

$$\sum \dot{E}x_{heat} - \sum \dot{E}x_{work} + \sum \dot{E}x_{mass,i} - \sum \dot{E}x_{mass,o} = \sum \dot{E}x_{dest} \quad (5)$$

The velocity form of the general exergy balance is:

$$\Sigma\left(1 - \frac{T_\infty}{T_w}\right)\dot{Q} - \dot{W} + \Sigma\dot{m}_i\psi_i - \Sigma\dot{m}_o\psi_o = \dot{E}x_{dest} \quad (6)$$

where ψ_i and ψ_o are given as:

$$\psi_i = (h_i - h_e) - T_\infty(s_i - s_e) \quad (7a)$$
$$\psi_o = (h_o - h_e) - T_\infty(s_o - s_e) \quad (7b)$$

When Eq.s (7a) and (7b) are replaced in Eq. (6), the equation is rearranged as follows [25].

$$\left(1 - \frac{T_\infty}{T_w}\right)\dot{Q} - \dot{m}(h_o - h_i) - T_\infty(s_o - s_i) = \dot{E}x_{dest} \quad (8)$$

where $\dot{Q}$ is the solar energy absorbed by the collector surface:

$$\dot{Q} = I(\tau\alpha)A_c \quad (9)$$

The enthalpy difference and entropy difference of the air in the collector can be written as follows.

$$\Delta_h = h_o - h_i = C_p(T_o - T_i) \quad (10)$$
$$\Delta s = s_o - s_i = C_p \ln\frac{T_o}{T_i} - R\ln\frac{P_o}{P_i} \quad (11)$$

By substituting Eqs (9), (10) and (11) into Eq. (8):

$$\left(1-\frac{T_\infty}{T_w}\right)I(\tau\alpha)A_c-\dot{m}C_p(T_o-T_i)+\dot{m}C_pT_\infty\ln\frac{T_o}{T_i}-\dot{m}RT_\infty\ln\frac{P_o}{P_i}=\dot{E}x_{dest} \quad (12)$$

where $\dot{E}x_{dest}$ is defined as irreversibility:

$$\dot{E}x_{dest}=T_\infty\dot{S}_{gen} \quad (13)$$

Then the exergy efficiency can be found by:

$$\eta_{II}=\frac{\dot{E}_{xo}}{\dot{E}_{xi}}=\frac{m[h_o-h_i-T_\infty(s_o-s_i)]}{\left(1-\frac{T_\infty}{T_w}\right)\dot{Q}} \quad (14)$$

The bulk temperature is used to choose thermophysical properties of air.

Uncertainty Analysis

In this study, the uncertainties in the measured values are evaluated using the Kline and McClintock [26] methodology. This method offers a structured and reliable approach for quantifying measurement uncertainties, ensuring the accuracy and credibility of the experimental results. According to this method, in a measurement with *n* independent variables, *R* is the dimension to be measured; x_1, x_2, x_3, …, x_n are the variables affecting the measurement; and ω_1, ω_2, ω_3, …, ωn are the uncertainties related to the independent variables.

$$\omega_R=\sqrt{\left(\frac{\partial R}{\partial x_1}\omega_1\right)^2+\left(\frac{\partial R}{\partial x_2}\omega_2\right)^2+\left(\frac{\partial R}{\partial x_3}\omega_3\right)^2+.+\left(\frac{\partial R}{\partial x_n}\omega_n\right)^2} \quad (15)$$

The independent parameters measured during the experiments included the outlet and inlet air temperatures, air velocity, solar radiation and ambient temperature. According to the instruments' catalog information the accuracy values of the thermocouples, anemometer and pyrometer are 0.018 °C, with ±2%, and 1% respectively. Hence the total uncertainties in estimating the dependent parameters are 4.5% for the mass flow rate of air, 1.8% for the thermal efficiency and 2% for the 2nd law efficiency.

RESULTS AND DISCUSSIONS

One effective method to enhance heat extraction from the absorber surface is to introduce flow obstacles into the air path. These obstacles, placed above the absorber surface, promote turbulence within the collector and consequently improve efficiency with minimal thermal loss. In this study, scourers were placed both above and below the absorbing surface in Collector T1 and T2 to achieve higher efficiency. This design enables a double-pass airflow, which, compared to single-pass airflow, increases the heat transfer area and turbulence, further improving collector efficiency. The findings suggest that stainless steel scourers present a practical and scalable solution for enhancing solar air collector performance, especially in applications such as residential heating, industrial drying, and greenhouse thermal management.

Graphs are used to display the experimental results and computed values. These graphs illustrate the temperature distribution obtained from thermocouples placed at regular intervals on the absorber surface over time, the variation in efficiency, and the changes in air temperature at the collector's input and output for mass flow rates of 0.025 kg/s and 0.05 kg/s.
The first-law efficiencies, namely the energy efficiencies of the three collector types over time, are presented in Fig. 3a and Fig. 3b for air mass flow rates of 0.025 kg/s and 0.05 kg/s, respectively. According to the bar graphs, at an air mass flow rate of 0.025 kg/s, the maximum energy efficiency values for T1, T2, and T3 are 62%, 56%, and 49%, respectively. When the air mass flow rate is increased to 0.05 kg/s, these efficiencies rise to 74%, 63%, and 62%, respectively. As the air mass flow rate increases, the temperature rise across the collector decreases, which leads to a reduction in absorber surface temperature, thereby minimizing thermal losses to the ambient environment and enhancing overall efficiency.

T3, which lacks turbulence-inducing surface elements, consistently demonstrates the lowest efficiency among all configurations. In contrast, T1 outperforms both T2 and T3, owing to its distinct absorber surface geometry. The superior performance of the T1 configuration is attributed to its irregular and densely packed distribution of stainless steel scourers, which significantly enhances turbulence within the collector's airflow. This elevated turbulence disrupts the thermal boundary layer, thereby increasing the convective heat transfer coefficient and improving the thermal energy exchange between the air and the absorber surface. Moreover, the placement of scourers on both sides of the absorber plate enables a dual-pass airflow mechanism that effectively enlarges the heat transfer surface area. This configuration not only reduces thermal losses but also promotes a more uniform temperature distribution across the collector surface, ultimately improving both energy and exergy efficiencies. These findings align with previous studies by Esen [10] and Akpınar and Koçyiğit [11], who also reported enhanced thermal performance with the integration of turbulence-inducing features in solar air collector designs.

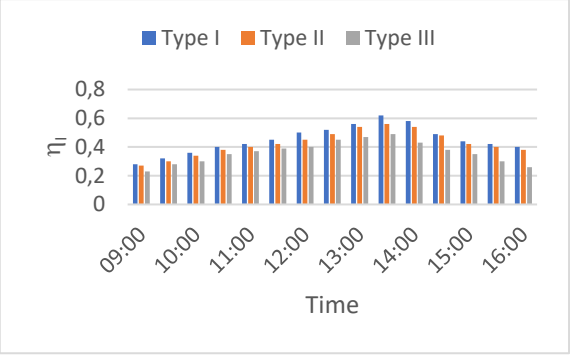

a)

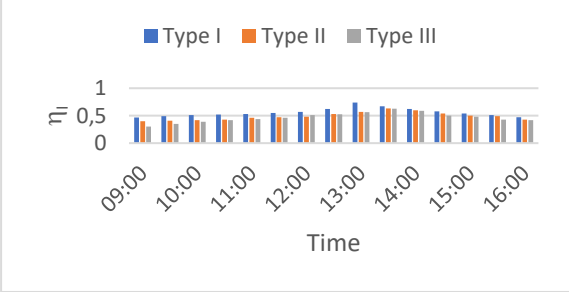

b)

Fig. 3 Variation of thermal efficiency over time for different types of absorbing surfaces **a**) $\dot{m} = 0.025\ kg/s$, **b**) $\dot{m} = 0.05\ kg/s$

Exergy analysis is utilized to identify the system's irreversible processes and assess how these destructive processes impact overall performance. This analysis is conducted for each absorbing surface, with calculations performed for destroyed exergy (irreversibility), exergy loss, and exergy efficiency. The max and min values for each parameter are summarized in Table 1. Exergy losses may occur due to thermal dissipation and optical inefficiencies [9]. In present study the highest lost exergy is seen when using the T3 collector (71.34% for 0.025 kg/s). The lowest lost exergy is obtained when T1 collector is used (34.2% for 0.05 kg/s). It is important to note that, under certain operating conditions, the exergy efficiency was observed to be slightly higher than the thermal efficiency. This outcome can be attributed to reduced irreversibility and lower entropy generation in configurations such as T1, where enhanced turbulence improves the quality of heat transfer. Since exergy analysis accounts not only for the quantity but also the quality of energy, the effective utilization of high-grade thermal energy can lead to higher exergy efficiency under favorable conditions.

Furthermore, the results indicate that the highest exergy loss occurs in the flat plate absorber surface (i.e., the collector without scourers), primarily due to significant thermal losses. The main contributors to energy destruction in SAH systems include heat transfer between the absorber and the environment, radiation losses to ambient air, and pressure drop within the collector duct [9]. These factors collectively reduce the overall system performance. The extent of energy destruction becomes particularly significant during midday, when absorber surface temperatures peak and thermal interactions intensify. Among the three collector configurations, the T1 design exhibits the highest levels of exergy destruction, which highlights the thermal management challenges associated with complex surface geometries. This limitation stems from its partial inability to utilize the absorbed solar energy efficiently. Therefore, there remains a need for further improvements in absorber geometry and system integration to enhance both energy and exergy performance in SAH applications.

Table 1. Exergy analysis

T1				
Flowrate $\dot{m}$, kg/s	0.025		0.05	
	Min.	Max.	Min.	Max.
Exergy loss, %	50.00	67.94	34.20	44.35
Irreversibility $\dot{E}x_{dest}$, kW	0.225	0.255	0.249	0.355
Exergy efficiency η_{II}, %	27.8	72	52	89
T2				
Flowrate $\dot{m}$, kg/s	0.025		0.05	
	Min.	Max.	Min.	Max.
Exergy loss, %	53.14	65.00	48.01	51.42
Irreversibility $\dot{E}x_{dest}$, kW	0.221	0.287	0.180	0.264
Exergy efficiency η_{II}, %	32	64	42	59
T3				
Flowrate $\dot{m}$, kg/s	0.025		0.05	
	Min.	Max.	Min.	Max.
Exergy loss, %	66.98	71.34	48.11	64.28
Irreversibility $\dot{E}x_{dest}$, kW	0.173	0.236	0.265	0.285
Exergy efficiency η_{II}, %	25	54	32	70

It is important to note that the scourers have a significant impact on the system's energy and exergy efficiency. Regardless of the air mass flow rate, T1 yields the highest exergy efficiency, while T3 exhibits the lowest under most conditions. Fig. 4a and Fig. 4b display the hourly energy efficiencies for $\dot{m}$ = 0.025 kg/s and $\dot{m}$ = 0.05 kg/s, respectively. For the flat absorber plate (T3), the average daily exergy efficiencies are 40% and 51%, respectively. However, in the presence of scourers, these values improve by 10–15%, reaching 50% and 66%, respectively, for $\dot{m}$= 0.025 kg/s and $\dot{m}$= 0.05 kg/s.

Although T2 includes surface roughness to enhance heat transfer, the increased flow resistance it introduces can lead to higher entropy generation. In contrast, the smoother surface of T3 results in lower pressure drop and less irreversibility, which may explain its slightly higher exergy efficiency compared to T2 under some conditions. This highlights the delicate trade-off between enhanced turbulence and fluid friction losses when evaluating exergy performance. As outlined, the main aim of this study is to evaluate the performance of stainless steel scourers attached to the absorber plate of a solar collector. The findings reveal that absorber surfaces equipped with scourer-type obstacles achieve higher energy and exergy efficiencies compared to flat surfaces. A summary of exergy and energy efficiencies reported in previous publications is presented in Table 2. It should be noted that direct comparisons with other studies are difficult due to variations in experimental and structural conditions. Nevertheless, the results of this experiment demonstrate strong agreement with the trends observed in the literature.

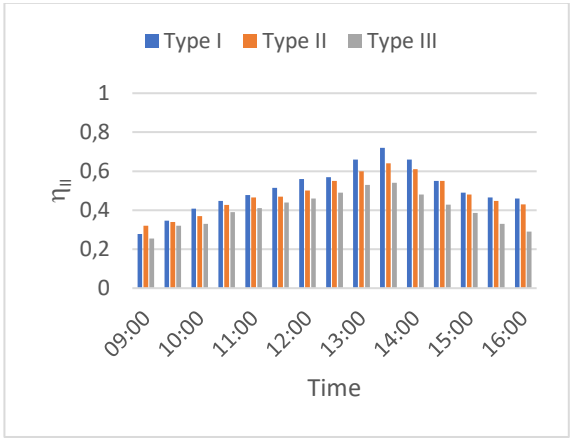

a)

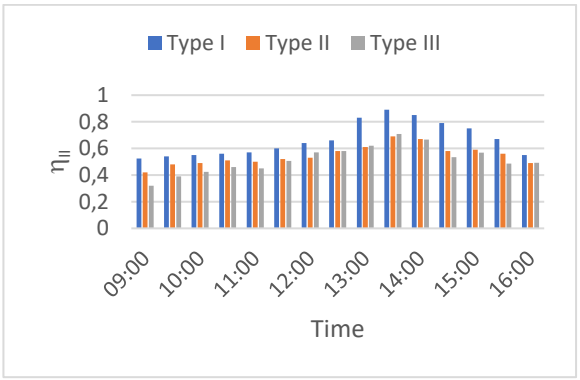

b)

Fig. 4 Variation of exergy efficiency over time for different types of absorbing surfaces **a**) $\dot{m} = 0.025\ kg/s$, **b**) $\dot{m} = 0.05\ kg/s$

Table 2 Comparison to the literature

	Absorber type	Energy efficiency %	Exergy efficiency %
Ucar and Inallı [14]	Flat single-pass	30.5	35.61
	Finned surface	35.2	49.37
Esen [10]	Flat double-pass	67.5	60.97
	Flat single-pass	48.12	33.83
Akpinar and Kocyigit [11]	Flat single-pass	25.51	10.15
	Rectangular obstacles	50.55	33.96
Present work	Stainless steel scourers	46-74	55.04

As shown in Table 2, the energy efficiencies achieved in this study, particularly for T1, exceed those of flat single-pass collectors studied by Ucar & İnallı [14] and are comparable to the double-pass systems analyzed by Esen [10]. The T1 design, which incorporates a complex arrangement of stainless steel scourers, achieves a maximum energy efficiency of 74% and an exergy efficiency of 66%, showcasing its ability to optimize heat transfer while minimizing thermal losses. Similar trends have been observed in studies such as Ali et al. [27], where passive flow control methods such as optimizing turbulence patterns demonstrated significant efficiency improvements in solar thermal systems.

The incorporation of turbulence-inducing elements in the form of scourers has proven effective in enhancing the thermal performance of SAHs. As Hroub et al. [28] emphasized, increasing the absorber surface area through innovative designs significantly reduces thermal losses and enhances efficiency, a principle also observed in this study. This complements the findings of Karim & Hawlader [16], who noted that V-corrugated and finned collectors outperformed flat plate designs by optimizing turbulence and heat transfer coefficients, similar to the enhancements seen with T1 in this study. These results confirm the critical role of obstacle design and complexity in improving thermal system performance.

Additionally, Sanaka et al. [29] demonstrated that sustainable, high-conductivity materials significantly improve absorber performance in solar air collectors, offering insights into the benefits of the stainless steel scourers used in this study. Such strategies align with the double-pass airflow designs of T1 and T2 tested here, where airflow paths above and below the absorber plate maximize heat transfer. Yeh et al. [18] also emphasized the benefits of such configurations, further validating the effectiveness of the T1 and T2 designs in this context.

The findings from this study highlight that innovative absorber surface designs, such as those tested here, can achieve superior thermal performance while maintaining simplicity and scalability. The stainless steel scourer configuration offers a practical and cost-effective solution for residential and industrial applications, particularly in regions with high solar radiation. Moreover, as noted by Ali et al. [27], integrating turbulence-enhancing designs can significantly boost system efficiency, providing opportunities for further optimization.

CONCLUSIONS

Maximizing heat extraction from the absorber surface of a solar air collector can be effectively achieved through the use of strategically placed airflow obstacles. These elements enhance internal turbulence, thereby increasing heat transfer rates and improving overall thermal efficiency while minimizing energy losses. In this study, stainless steel scourers were installed both above and below the absorber plate in T1 and T2 configurations, forming a double-pass airflow system. This design enlarges the heat transfer area, induces beneficial turbulence, and markedly improves collector performance.

The study evaluated three different collector types distinguished by their absorber surface geometries. T1 features a complex and irregular wire arrangement, T2 includes a simpler row-based configuration, while T3 employs a flat absorber surface with no enhancement elements. Experimental tests were conducted at air mass

flow rates of 0.025 kg/s and 0.05 kg/s. The findings show that T1 outperforms T2 in both energy and exergy efficiencies, primarily due to its irregular scourer placement that promotes turbulence, enhances heat transfer, raises absorber temperatures, and reduces thermal losses. Conversely, T3 exhibits the lowest efficiency owing to its flat geometry, which limits turbulence and reduces effective heat transfer area.

When compared to data reported in the literature, the study confirms that well-designed collectors like T1 can achieve notable efficiency, with energy efficiencies reaching up to 74%, a level considered satisfactory for solar air collectors. However, the flat-plate absorber surface (T3) exhibited the greatest irreversibility, as only a small portion of the absorbed solar energy contributes effectively to the exergy analysis. The findings of this study have notable implications for industrial applications, particularly in the fields of sustainable thermal energy systems. The enhanced thermal and exergy performance observed in the T1 and T2 configurations indicates their suitability for practical use in low- to medium-temperature industrial processes. Potential applications include agricultural drying of fruits, vegetables, and herbs; greenhouse heating; and preheating of ventilation air in residential or industrial buildings. These configurations offer the potential for improved energy efficiency and reduced operational costs, contributing to cleaner and more cost-effective thermal energy solutions in various sectors.

Nomenclatures

Symbol	Description	Unit
$\dot{m}$	Air mass flow rate	kg/s
h	Specific enthalpy	J/kg
u	Internal energy	J/kg
U	Overall heat transfer coefficient	W/(m²·K)
L	Collector length	m
W	Collector width	m
V	Air velocity	m/s
Re	Reynolds number	–
Nu	Nusselt number	–
Pr	Prandtl number	–
k	Thermal conductivity coefficient	W/(m·K)

REFERENCES

[1] Varun, Saini R. P., Singal S. K. A review on roughness geometry used in SAHs, Solar Energy, 81, 1340–1350,2007.
[2] Ekramian E., Etemad S. Gh., Haghshenasfard M. Numerical analysis of heat transfer performance of flat plate solar collectors, Journal of Fluid Flow Heat and Mass Transfer, 1, 38–46,2014.
[3] Kalogirou S. A. Environmental benefits of domestic solar energy systems. *Solar Energy*, 85(1), 118-133, 2011.
[4] Pathak P. K., Chandra P., Raj G. Energy and exergy analysis of corrugated plate solar collector by forced convection using two different absorber plate material, Heat and Mass Transfer, 57,565–581,2021.
[5] Esen H., Ozgen F., Esen M., Sengur A. Artificial neural network and wavelet neural network approaches for modelling of a SAH, Expert Systems with Applications, 36, 11240–11248,2009.
[6] Gürtürk M., Benli H., Ertürk N. K. Effects of different parameters on energy – exergy and power conversion efficiency of PV modules, Renewable and Sustainable Energy Reviews, 92,426–439,2018.
[7] Darici S., Kilic A. Comparative study on the performances of solar air collectors with trapezoidal corrugated and flat absorber plates, Heat and Mass Transfer, 24, 1–1, 2020.
[8] Facão J. Optimization of flow distribution in flat plate solar thermal collectors with riser and header arrangements, Solar Energy,120,104–112,2015.
[9] Avargani V. M., Zendehboudi S., Rahimi A., Soltani S. Comprehensive energy, exergy, enviro-exergy, and thermo-hydraulic performance assessment of a flat plate SAH with different obstacles, Applied Thermal Engineering, 203, 117907,2022.
[10] Esen H. Experimental energy and exergy analysis of a double-flow SAH having different obstacles on absorber plates, Building and Environment, 43, 1046–1054, 2008.
[11] Akpinar E., Koçyiğit F. Energy and exergy analysis of a new flat-plate SAH having different obstacles on absorber plates, Applied Energy, 87, 3438–3450, 2010.
[12] Ozgen F., Esen M., Esen H. Experimental investigation of thermal performance of a double-flow SAH having aluminium cans, Renewable Energy, 34, 2391–2398, 2009.
[13] Arabhosseini A., Samimi-Akhijahani H., Motahayyer M. Increasing the energy and exergy efficiencies of a collector using porous and recycling system, Renewable Energy, 132, 308–325,2019.
[14] Ucar A., Inalli M. Thermal and exergy analysis of solar air collectors with passive augmentation techniques, International Communications in Heat and Mass Transfer, 33, 1281–1290, 2006.
[15] Albizzati E. D. Solar collector for air heater, International Solar nEnergy Society, 22, 663–666,2000.
[16] Karim M. A., Hawlader M. N. A. Performance investigation of flat plate, v-corrugated and finned air collectors,Energy,31,452–470,2006.
[17] Moummi N., Youcef Ali S., Moummi A., Desmons J. Y. Energy analysis of a solar air collector with rows of fins, RenewableEnergy,29,2053–2064,2004.
[18] Yeh H. M., Ho C. D., Hou J. Z. The improvement of collector efficiency in SAHs by simultaneously air flow over and under the absorbing plate, Energy, 24, 857–871, 1999.
[19] Sahu M. M., Bhagoria J. L. Augmentation of heat transfer coefficient by using 90° broken transverse ribs on absorber plate of SAH, Renewable Energy, 30, 2057–2073, 2005.
[20] Alvarez G., Arce J., Lira L., Heras M. R. Thermal performance of an air solar collector with an absorber plate made of recyclable aluminium cans, Solar Energy, 77, 107–113,2004.
[21] Kreith F., Kreider J. F. Principles of Solar Engineering, McGraw-Hill,NewYork,1978.
[22] Ghoneim A. A. Performance optimization of solar collector equipped with different arrangements of square-celled honeycomb, International Journal of Thermal Sciences, 44, 95–105,2005.
[23] Ozgen F., Dayan A. Energy analysis of a SAH with an absorber plate made of porous material, Thermal Science,25,333–337,2021.
[24] Can O. F., Celik N., Ozgen F., Kistak C., Taskiran A. Experimental and numerical analysis of the solar collector with stainless steel scourers added to the absorber surface, Applied

Sciences-Basel, 14, Article number: 2629,2024.
[25] Torres-Reyes E., Navarrete-Gonzalez J. J., Zaleta-Aguilar A., Cervantes-de Gortari J. G. Optimal process of solar to thermal energy conversion and design of irreversible flat-plate solar collectors, Energy, 28, 99–113,2003.
[26] Kline S. J., McClintock F. A. Describing uncertainties in single-sample experiments, Mechanical Engineering, 75, 3–8, 1953.
[27] Ali, M. H., Kurjak, Z., Beke, J. The Effect of Forced Airflow Inside the Solar Chimney on the Photovoltaic Module Power Generation. 29th Workshop on Energy and Environment, 2023.
[28] Hroub, Q., Drira, Y., Jribi, S., Bentaher, H. Advancing Solar Thermal Energy Systems: Comparative Study of Low-Cost Receivers in Parabolic Trough Collectors. Journal of Renewable and Sustainable Energy, 16(6), 063704, 2024.
[29] Sanaka, S. P., Mareedu, N. D., et al. Characterization of Sustainable Solar Absorbing Materials for Solar Thermal Applications. IEEE Xplore, 2024.